

Synthesis and Chain-Length Dependent Properties of Monodisperse Oligo(9,9-di-*n*-octylfluorene-2,7-vinylene)s

Qin Liu, Wenming Liu, Bing Yao, Hongkun Tian, Zhiyuan Xie, Yanhou Geng,* and Fosong Wang

State Key Laboratory of Polymer Physics and Chemistry, Changchun Institute of Applied Chemistry, Graduate School of Chinese Academy of Sciences, Chinese Academy of Sciences, Changchun 130022, P. R. China

Received December 7, 2006; Revised Manuscript Received January 29, 2007

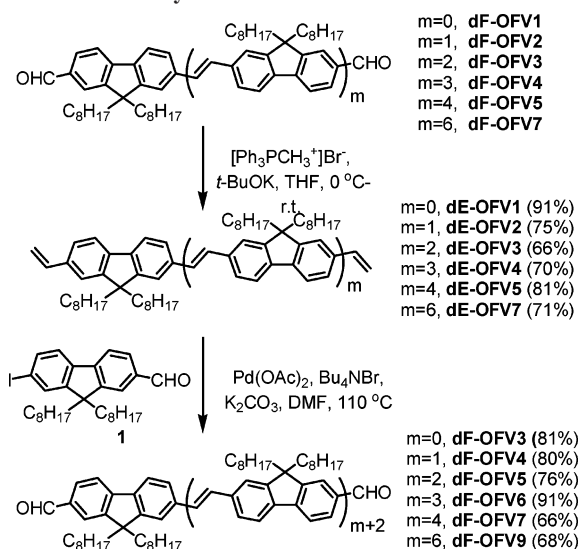
ABSTRACT: A series of monodisperse oligo(9,9-di-*n*-octylfluorene-2,7-vinylene)s (OFVs) with fluorene units up to 11 has been synthesized following a divergent approach. Chain length was found to affect not only photophysical properties but also thermal properties. Absorption and photoluminescence spectra are red-shifted with increasing chain length. The effective conjugated length has been extrapolated to be as long as 19 fluorene vinylene units, indicative of a well-conjugated system. With the number of fluorene units >5, the oligomers exhibit nematic mesomorphism. Glass transition temperature (T_g) and clearing point temperature (T_c) increase with increasing molecular length and with those of **OFV11** up to 71 and 230 °C, respectively. The oligomers can form uniform films by solution casting for fabrication of light-emitting diodes. With a device structure of ITO/PEDOT:PSS/**OFV11**/Ca/Al, a current efficiency of 0.8 cd·A⁻¹ at a brightness of 1300 cd·m⁻² along with a maximum brightness of 2690 cd·m⁻² have been realized. This performance is notably superior to that of the corresponding polymer.

Introduction

Conjugated polymers have attracted particular attention due to their various applications in optoelectronic devices, e.g., light-emitting diodes (LEDs), solar cells and thin-film transistors (TFTs). Poly(*p*-phenylenevinylene)s (PPVs) and poly(9,9-dialkylfluorene)s (PFs) are so far considered to be the most promising conjugated polymers for polymer light-emitting diodes.¹ By combining the structural features of PPVs and PFs, poly(9,9-dialkylfluorenyl-2,7-vinylene)s (PFVs) have recently been synthesized by means of Heck coupling reaction,² Gilch polymerization,³ Horner–Emmons reaction⁴ and acyclic diene metathesis polymerization,⁵ and these polymers exhibit promising thermal stability and high photoluminescence quantum yield. However, it seems that the photophysical and thermal properties of the resulting polymers depend on synthetic method, probably due to different content of defects.^{3c,5} This prevents one from fully characterizing the properties and evaluating the potentials of PFVs.

Monodisperse conjugated oligomers (MCOs) are characterized by uniformity, ease of purification and well-defined structures.⁶ Hence, MCOs have been widely studied for understanding of the intrinsic properties of different conjugated systems, establishment of chain length-property correlations, fabrication of high performance optoelectronic devices, and application as molecular wires.^{6,7} However, synthesis of long MCOs is still a great challenge and only few examples have been reported.^{8–13} Recently, fluorene-based MCOs have received particular interest.^{8,14–16} Oligo(9,9-dialkylfluorene)s (OFs) with different alkyl chains and chain length up to 16 repeating units have been synthesized and used in fabrication of LEDs and TFTs, and exhibited somewhat better device performance than their polymeric counterparts.^{8,14,15} Tsutsui et al. have also reported the synthesis and photophysical properties of oligo(fluoreneethynylene)s with fluorene units up to 5.¹⁶ In

Scheme 1. Synthesis of **dE-OFV_n** and **dF-OFV_n**



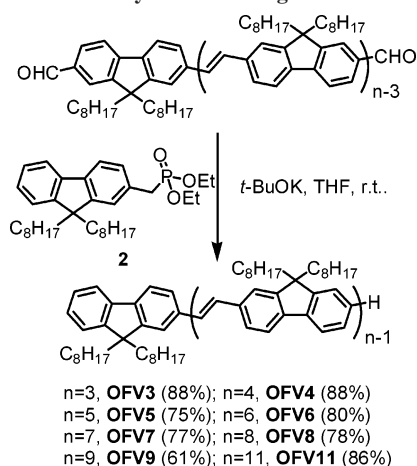
current paper, oligo(9,9-di-*n*-octylfluorene-2,7-vinylene)s (OFVs) with different length were synthesized, and their photophysical, thermal and electroluminescent properties were studied in detail.

Results and Discussion

Synthesis and Characterization. In general, MOCs are synthesized with iterative divergent/convergent strategy for ease of purification, especially for synthesis of long-chain MOCs.^{6a} However, divergent approach could significantly reduce workload, e.g., fewer intermediates required, once the difficulties in purification process are solved. Here, we proposed a divergent approach as shown in Scheme 1 and 2 for successful synthesis of OFVs with fluorene units up to 11. First, the diformyl-oligo(9,9-di-*n*-octylfluorene-2,7-vinylene)s (**dF-OFV_n**, in which *n* represents the number of fluorene unit) were converted to diethenyl-oligo(9,9-di-*n*-octylfluorene-2,7-vinylene)s (**dE-OFV_n**, in which *n* represents the number of fluorene unit) via typical

* To whom correspondence should be addressed. E-mail: yhgeng@ciac.jl.cn.

Scheme 2. Synthesis of Oligomers OFVn



Wittig reaction in a yield of 70–91%. Second, two fluorene units were introduced through Heck coupling¹⁷ to realize chain growth and afford two fluorene-units longer conjugated molecules terminated with $-\text{CHO}$ groups in a yield of 66–91%. Finally, these formyl end-capped oligomers were converted to target molecules (**OFVn**) by means of Horner–Emmons reaction in a good yield (61–88%), as shown in Scheme 2. With this approach (polar–nonpolar), the product in each step can be easily purified by column chromatography on silica gel due to significantly different polarity between the product and the reactants/byproducts. Moreover, only two other intermediates (compounds **1** and **2**) were used in the whole process. Our results indicate that the divergent approach can also be very effective in the synthesis of long MCOs with the appropriate synthesis strategy.

The structures of oligomers **OFVn** were confirmed by ^1H NMR, elemental analysis, MALDI–TOF mass spectroscopy, and gel permeation chromatography (GPC) with polystyrene as the standard. ^1H NMR spectra of all oligomers are consistent with their structures and no peak at ~ 6.5 ppm corresponding to protons in *cis*-double bonds ($-\text{CH}=\text{CH}-$) was observed,⁵ indicating that all ethenyl groups in **OFVn** adopt the *trans*-conformation. Figure 1a shows the aromatic region of ^1H NMR spectra of **OFV3**, **OFV8**, and **OFV11** along with the assignment as examples. The ratios of three groups of peaks in the range of 7.66–7.74, 7.50–7.61, and 7.27–7.41 ppm are 6.0:8.2:10.5, 16.0:26.4:19.6, and 22:40:25.6 for **OFV3**, **OFV8**, and **OFV11**, respectively, consistent with the expected values of 6:8:10, 16:28:20, and 22:40:26. The calculated molecular mass, the molecular weight measured by MALDI–TOF mass spectroscopy and the weight-average molecular weight measured by GPC are listed in Table 1. Figure 1b shows representative MALDI–TOF mass spectra of OFVs. Meanwhile, GPC profiles confirmed that all OFVs are monodisperse (GPC profiles please see Supporting Information). These indicate that all these oligomers are composed of single component. It should be noted that the M_w from GPC measurements deviates more and more from real molecular weights with increasing molecular length, indicative of different geometry of **OFVn** molecules from polystyrene, a random-coil polymer. This inflation of molecular weights in GPC measurements vs polystyrene standard is a general phenomenon for rodlike long conjugated oligomers and polymers.^{9,18}

Thermotropic Properties. Thermotropic properties of **OFVn** as characterized by differential scanning calorimetry (DSC) and polarizing optical microscopy (POM) are summarized in Table 1, and Figure 2 shows the second heating DSC scans of

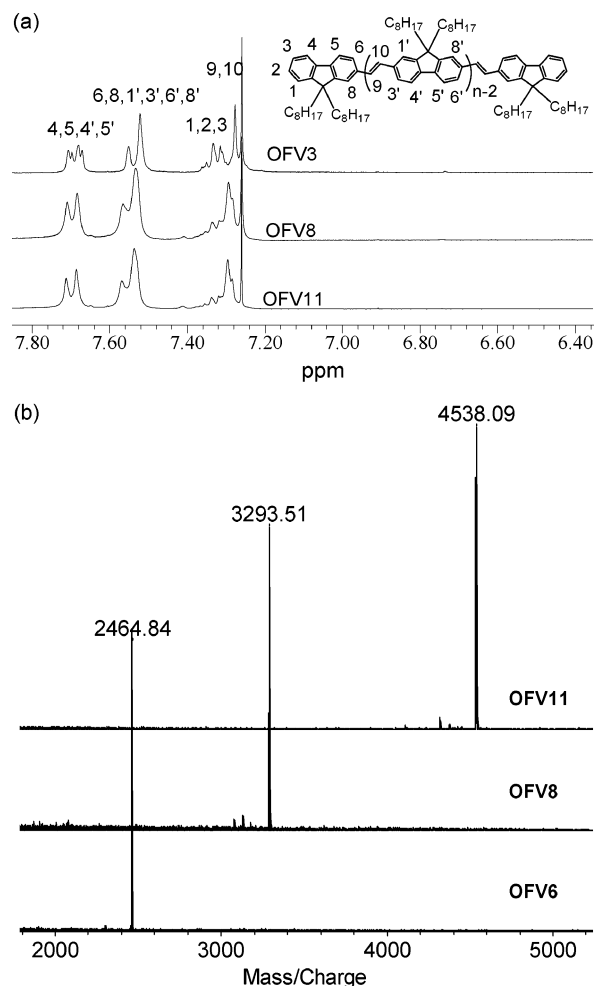


Figure 1. ^1H NMR (a) and MALDI–TOF mass (b) spectra of representative **OFVn**.

Table 1. Calculated Molecular Weight (M_{cal}), Molecular Weight Measured by Mass Spectroscopy (M_{MS}), Weight Average Molecular Weight (M_w) Measured by GPC, Glass Transition Temperature (T_g), Clearing Point Temperature (T_c), and Enthalpy of Nematic–Isotropic Transition of **OFVn**

compound	M_{cal}	M_{MS}^a	M_w	PDI	T_g^b ($^{\circ}\text{C}$)	T_c^b ($^{\circ}\text{C}$)	ΔH_c^b ($\text{J} \times \text{g}^{-1}$)
OFV2	803.65	803.55	900	1.01			
OFV3	1218.98	1218.93	1400	1.01			
OFV4	1633.31	1633.18	2000	1.02	23		
OFV5	2047.64	2048.56	2700	1.02	31		
OFV6	2462.97	2462.88	3600	1.02	44	106	0.76
OFV7	2877.30	2878.16	4500	1.02	54	135	0.72
OFV8	3291.63	3292.50	5500	1.02	56	148	0.33
OFV9	3706.96	3707.88	6500	1.02	65	180	0.25
OFV11	4535.62	4537.02	8800	1.02	71	230	0.62

^a Matrix is 2,5-dihydroxybenzoic acid. ^b Measured by DSC with a heating rate of $10^{\circ}\text{C} \cdot \text{min}^{-1}$.

OFV4–9 and **OFV11**. It was found that the oligomers longer than **OFV5** are nematic mesomorphism. At a scan rate of $10^{\circ}\text{C} \cdot \text{min}^{-1}$, all oligomers longer than **OFV5** display a glass transition temperature (T_g) and a clearing point (T_c), which increase with increasing molecular length. For instance, T_g and T_c of **OFV11** increase to 71 and 230°C from 44 and 106°C of **OFV6**, respectively. The typical nematic textures, e.g., threaded textures and droplets, as shown in Figure 3, can be observed under hot-stage POM of a micrometer-thick film on a glass slide with a coverslip for oligomers longer than **OFV5**. An endothermal peak above T_g was also observed in DSC heating scans

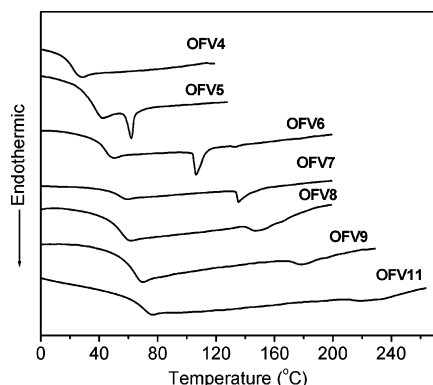


Figure 2. The second DSC heating scans of **OFV n** ($n \geq 4$) with a heating rate of $10\text{ }^{\circ}\text{C}\cdot\text{min}^{-1}$.

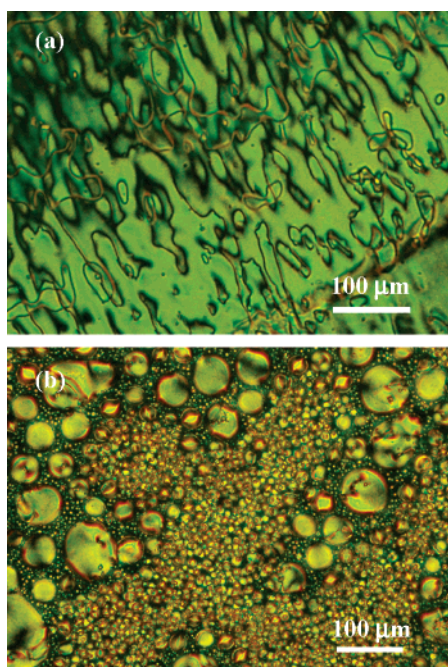


Figure 3. Nematic threaded textures of **OFV7** (a) at $100\text{ }^{\circ}\text{C}$ and droplets of **OFV11** (b) at $220\text{ }^{\circ}\text{C}$ upon cooling observed under hot-stage polarizing optical microscope.

of **OFV5**. However, POM observations indicate that the anisotropic state of **OFV5** is not nematic, but crystalline phase or higher order mesophase. In previous report, Hwang et al. also studied the thermal properties of poly(9,9-di-*n*-octylfluorene-2,7-vinylene) (PFV8) prepared by Gluch polymerization, however, no mesophase formation was observed.^{3a} This observation further corroborates the advantages of MCOs on studying the intrinsic properties of the conjugated systems.

As indicated in Table 1 and Figure 2, similar to the case of OFs,^{15a} the T_g values tend to level off as the chain length increases and exhibit $1/m$ dependence following the equation: $T_g = 88.0 - 200.2m^{-1}$, in which m is the number of fluorene vinylene units. This indicates that the reasonable T_g of the corresponding polymer should be around $90\text{ }^{\circ}\text{C}$. This value is significantly lower than the reported T_g of PFV8 containing 10–15% saturated defects,^{3c} but $\sim 20\text{ }^{\circ}\text{C}$ higher than that of poly-(9,9-di-*n*-hexylfluorene-2,7-vinylene) (PFV6) from Heck coupling as measured by thermomechanical analysis.^{2a}

Photophysical Properties. To evaluate the chain-length dependent photophysical properties of OFVs, solution absorption and photoluminescence (PL) spectra were measured in tetrahydrofuran (THF) with a concentration of $1 \times 10^{-5}\text{ mol}\cdot\text{L}^{-1}$

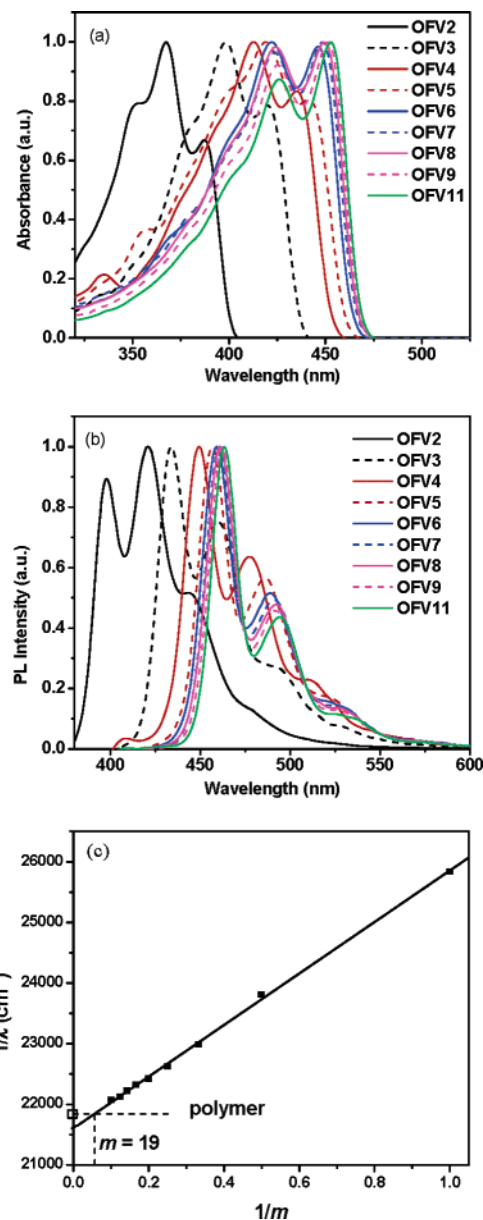


Figure 4. Solution absorption (a) and PL (b) spectra of **OFV n** as well as the plot of the wave number ($1/\lambda$) of the 0–0 absorption maximum vs $1/m$ (c), in which m is the number of fluorene vinylene units.

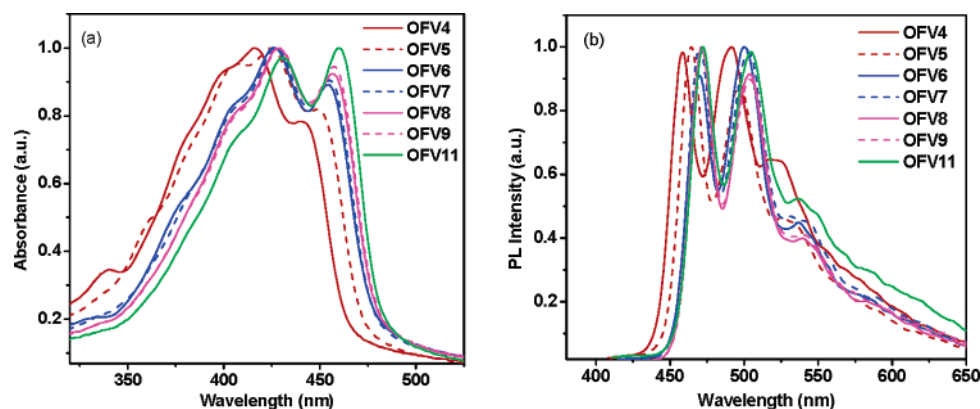
(fluorene unit), as shown in Figure 4, parts a and b. Absorption and emission maxima are listed in Table 2. All oligomers exhibit well-resolved absorption and PL spectra. With **OFV11** as an example, three absorption peaks at 453, 426, and 404 nm can be attributed to 0–0, 0–1, and 0–2 transitions, respectively, with corresponding emission peaks at 463, 494, and 526 nm. A 10–20 nm Stokes shift of OFVs, compared with the value of 30–40 nm of OFs and PFs,^{1e} and the well-resolved absorption spectra indicate that the conjugated molecules based on fluorenevinylene repeating unit are more rigid than OFs. Meanwhile, all OFVs exhibit a red-shifted absorption and PL spectra than OFs. The PL quantum yield (Φ) measured in THF with diphenylanthracene as a standard is in the range of 0.75–0.92, indicating that **OFV n** are also efficient emissive species.

Both absorption and emission spectra red-shift with increasing chain length. As shown in Table 2, the 0–0 absorption and PL maxima red-shift from 387 and 444 nm for **OFV2** to 453 and 526 nm for **OFV11**, respectively. However, the absorption maximum of **OFV11** is still 5 nm shorter than that of the “defect-free” PFV8, which shows the absorption maximum of

Table 2. Absorption (λ_{abs}) and PL (λ_{PL}) Maxima, HOMO/LUMO Energy Levels, PL Quantum Yield of OFVn

compound	λ_{abs} (nm)		λ_{PL} (nm)		HOMO ^b (eV)	LUMO ^c (eV)	Φ ^d
	solution ^a	film	solution ^a	film			
OFV2	351, 368, 387	358, 376, 398	398, 421, 444	406, 430, 458	−5.49	−2.41	0.75
OFV3	380, 398, 420	383, 400, 425	434, 460, 493	442, 476, 508	−5.35	−2.52	0.88
OFV4	393, 413, 435	398, 416, 441	450, 478, 511	458, 492, 517	−5.34	−2.60	0.88
OFV5	401, 419, 442	405, 424, 449	456, 483, 523	464, 496, 527	−5.33	−2.64	0.92
OFV6	401, 422, 446	405, 426, 454	459, 489, 522	470, 500, 537	−5.33	−2.65	0.80
OFV7	402, 424, 448	406, 427, 455	461, 491, 526	470, 503, 540	−5.32	−2.65	0.91
OFV8	403, 424, 450	407, 429, 457	461, 492, 526	472, 504, 540	−5.32	−2.65	0.86
OFV9	404, 425, 452	407, 429, 457	462, 492, 526	472, 504, 541	−5.32	−2.66	0.85
OFV11	404, 426, 453	410, 431, 460	463, 494, 526	472, 505, 537	−5.31	−2.66	0.85

^a Measured in anhydrous THF with a concentration of 1×10^{-5} mol·L^{−1}. ^b Calculated from cyclic voltammogram measurements in methylene chloride solution with concentration of 1×10^{-3} mol·L^{−1} (repeating unit). ^c Calculated from the HOMO level and UV–vis absorption edge. ^d Measured in THF with diphenylanthracene ($\Phi = 0.85$ in benzene²⁰) as a standard at excitation wavelength of 390 nm.

**Figure 5.** Film absorption (a) and PL (b) spectra of **OFVn**.

458 nm.⁴ This implies that fluorene vinylene conjugated systems have a significantly long effective conjugation length, especially while considering the molecular length of **OFV11** with extended chain conformation is already ~ 11 nm. From the plot of $1/\lambda$ of the 0–0 absorption maximum vs $1/m$ (Figure 4c), in which m represents the number of fluorene vinylene unit, the effective conjugation length of OFVs is extrapolated to be 19 repeating units, corresponding to an extended chain length of ~ 20 nm. The highest occupied molecular orbital (HOMO) and the lowest unoccupied molecular orbital (LUMO) energy levels, estimated by the combination of electrochemical and absorption measurements, are also listed in Table 2. The HOMO energy levels of **OFVn** are 0.3–0.5 eV higher than that of PFs (5.8 eV),¹⁹ which indicates easier hole-injection than PFs in the typical light-emitting diode structure.

Uniform films of **OFV4–9** and **OFV11** can be prepared via solution casting for film absorption and PL spectra measurements. As shown in Figure 5 and Table 2, in comparison with solution ones, both film absorption and PL spectra exhibit a ~ 10 nm red shift. Meanwhile, similar to the case in solution spectra, both absorption and emission spectra red-shift with increasing molecular length.

Electroluminescent Properties. To test the electroluminescent (EL) properties of OFVs, three oligomers, i.e., **OFV7**, **OFV9**, and **OFV11**, which have relative high T_g , were selected to fabricate LED with a device structure of ITO/poly(3,4-ethylenedioxythiophene):poly(styrene sulfonic acid) (PEDOT:PSS, 50 nm)/**OFVn** (70 nm)/Ca/Al. Device performance measurements were carried out in the air without any encapsulation. All the oligomers **OFV7**, **OFV9**, and **OFV11** emit greenish-blue electroluminescence as indicated by Commission Internationale de L'Eclairage (CIE) coordinates, which are (0.16, 0.33), (0.19, 0.39) and (0.18, 0.39) for **OFV7**, **OFV9**, and **OFV11**, respectively, with EL spectra similar to PL counterparts,

as shown in Figure 6a. Meanwhile, the EL spectra are almost independent of driving voltage. As shown in Table 3 and Figure 6b (with **OFV11** as an example), the devices turn on at a voltage of 2.5–3.0 V and achieve the maximum brightness at 6–8 V. The devices based-on **OFV11** exhibit the best device performance with a maximum brightness of 2690 cd·m^{−2} and a current efficiency of 0.8 cd·A^{−1} at a brightness of 1300 cd·m^{−2}. This efficiency is 5 times of that of the devices based-on polymer counterpart PFV8.³ The oligomers **OFV7** and **OFV9** exhibit inferior device performance than **OFV11** with current efficiency/maximum brightness of 0.08 cd·A^{−1}/362 cd·m^{−2} and 0.25 cd·A^{−1}/885 cd·m^{−2}, respectively. This may be ascribed to that **OFV11** can form more robust film due to higher molecular weight and T_g .

Conclusions

The series of monodisperse OFVs has been synthesized following the divergent approach to furnish the inside into the intrinsic properties of conjugated molecules based-on fluorene vinylene repeating unit and how chain length affects the thermotropic and optical properties. It is found that the divergent approach is very effective to synthesize OFVs with up to 11 fluorene units by alternatively introducing polar and nonpolar terminal groups into conjugated segments in chain growth process. OFVs are well-conjugated system and possess an effective conjugation length with 19 fluorene vinylene units. With the number of fluorene units > 5 , the oligomers are liquid crystalline and can form nematic mesophase. OFVs can be used to fabricate EL devices more efficient than their polymer counterparts. With a device structure of ITO/ PEDOT:PSS/ **OFV11**/Ca/Al, a maximum brightness of 2690 cd·m^{−2} and a current efficiency of 0.8 cd·A^{−1} at a brightness of 1300 cd·m^{−2} have been realized.

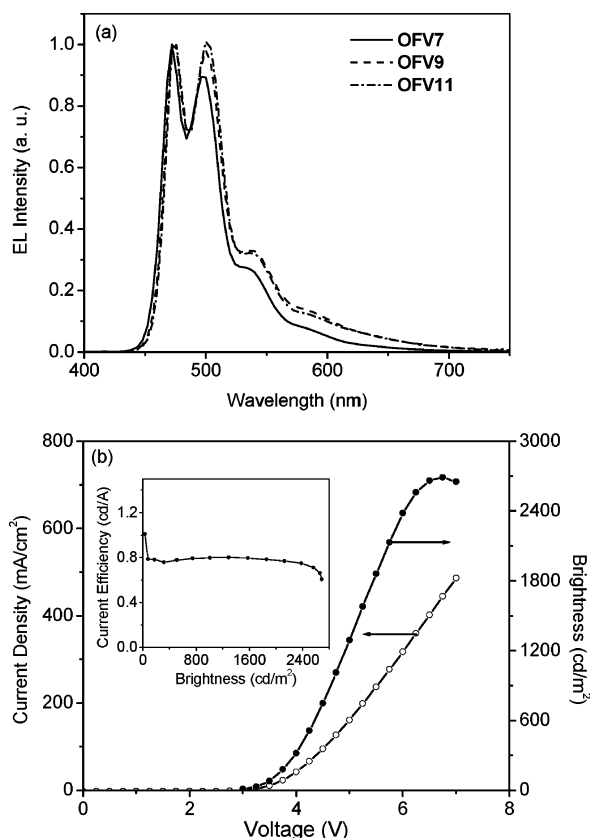


Figure 6. EL spectra of OFV7, OFV9, and OFV11 (a), and current density–voltage–brightness plots of device based on OFV11 (b). The inset shows the driving voltage dependence of current efficiency.

Table 3. Turn-on Voltage (V_{on}), Maximum Brightness (B_{max}), Current Efficiency (CE), External Quantum Efficiency (EQE), and CIE Coordinates of the Devices with the Configuration of ITO/PEDOT: PSS/OFV $_n$ /Ca/Al

compound	V_{on}^a (V)	B_{max} ($\text{cd}\cdot\text{m}^{-2}$)	CE ^b ($\text{cd}\cdot\text{A}^{-1}$)	EQE ^b (%)	CIE (x, y) ^b
OFV7	3.0	362	0.08	0.036	0.16, 0.33
OFV9	3.0	885	0.25	0.10	0.19, 0.39
OFV11	2.8	2690	0.80	0.30	0.18, 0.39

^a The voltage with a brightness of $3 \text{ cd}\cdot\text{m}^{-2}$. ^b The data at 5 V with a brightness of 247, 380, and $1300 \text{ cd}\cdot\text{m}^{-2}$ for OFV7, OFV9, and OFV11, respectively.

Experimental Section

Materials. Tetrahydrofuran (THF) and ethyl ether were distilled over sodium/benzophenone. *N,N*-Dimethylformamide (DMF) was distilled over CaH_2 under reduced pressure. Other reagents were used as received without further purification. The synthesis of OFV2 and other intermediates is included in the Supporting Information.

General Procedure for Synthesis of dE-OFV $_n$ by Wittig Reaction. Into a degassed mixture of dF-OFV $_n$ (1 equiv, $0.05 \text{ mol}\cdot\text{L}^{-1}$) and triphenylmethylphosphonium bromide (3 equiv) in anhydrous THF was added potassium *tert*-butoxide (8 equiv, 1.0 M solution in THF) at 0°C . The mixture was stirred for 12 h at room temperature, poured into water (100 mL), and extracted with petroleum ether ($3 \times 50 \text{ mL}$). The organic extracts were washed with brine, dried with anhydrous MgSO_4 , and then concentrated. The product was purified on a silica gel column with petroleum ether/dichloromethane as eluent.

2,7-Diethenyl-9,9-di-*n*-octylfluorene (dE-OFV1). A viscous colorless liquid was obtained in 85% yield. ^1H NMR (CDCl_3): δ (ppm) 7.62 (d, 2 H, $J = 10.8 \text{ Hz}$), 7.35–7.40 (m, 4 H), 6.80 (dd, 1 H, $J = 10.9 \text{ Hz}$, 17.6 Hz), 5.79 (d, 1 H, $J = 17.6 \text{ Hz}$), 5.25 (d, 1 H, $J = 10.8 \text{ Hz}$), 1.92–1.98 (m, 4 H), 0.91–1.28 (m, 20 H),

0.81 (t, 6 H, $J = 6.9 \text{ Hz}$), 0.51–0.70 (m, 4 H). Anal. Calcd for $\text{C}_{33}\text{H}_{46}$: C, 89.53; H, 10.43. Found: C, 89.40; H, 10.41.

1,2-Bis(2-ethenyl-9,9-di-*n*-octylfluorenyl)ethene (dE-OFV2). A pale yellow solid was obtained in 75% yield. ^1H NMR (CDCl_3 , 300 MHz): δ (ppm) 7.27–7.70 (m, 14 H), 6.84 (dd, 2 H, $J = 10.9 \text{ Hz}$, 17.6 Hz), 5.83 (d, 2 H, $J = 17.6 \text{ Hz}$), 5.29 (d, 2 H, $J = 10.9 \text{ Hz}$), 1.91–2.12 (m, 8 H), 0.95–1.36 (m, 40 H), 0.83 (t, 12 H, $J = 6.9 \text{ Hz}$), 0.57–0.75 (m, 8 H). Anal. Calcd for $\text{C}_{64}\text{H}_{88}$: C, 89.65; H, 10.35. Found: C, 89.59; H, 10.41.

2,7-Bis[2-(2-ethenyl-9,9-di-*n*-octylfluorenyl)ethenyl]-9,9-di-*n*-octylfluorene (dE-OFV3). A bright yellowish green solid was obtained in 66% yield. ^1H NMR (CDCl_3 , 300 MHz): δ (ppm) 7.27–7.68 (m, 38 H), 6.81 (dd, 2 H, $J = 10.9 \text{ Hz}$, 17.6 Hz), 5.81 (d, 2 H, $J = 17.6 \text{ Hz}$), 5.26 (d, 2 H, $J = 11.1 \text{ Hz}$), 1.88–2.12 (m, 12 H), 0.95–1.28 (m, 60 H), 0.80 (t, 18 H, $J = 6.9 \text{ Hz}$), 0.52–0.74 (m, 12 H). Anal. Calcd for $\text{C}_{95}\text{H}_{130}$: C, 89.70; H, 10.30. Found: C, 89.55; H, 10.55.

1,2-Bis[2-[2-(2-ethenyl-9,9-di-*n*-octylfluorenyl)ethenyl]-9,9-di-*n*-octylfluorenyl]ethene (dE-OFV4). A bright yellowish green solid was obtained in 70% yield. ^1H NMR (CDCl_3 , 300 MHz): δ (ppm) 7.28–7.70 (m, 30 H), 6.82 (dd, 2 H, $J = 10.9 \text{ Hz}$, 17.5 Hz), 5.81 (d, 2 H, $J = 17.6 \text{ Hz}$), 5.26 (d, 2 H, $J = 11.0 \text{ Hz}$), 1.90–2.14 (m, 16 H), 0.94–1.35 (m, 80 H), 0.80 (t, 24 H, $J = 6.9 \text{ Hz}$), 0.55–0.74 (m, 16 H). Anal. Calcd for $\text{C}_{126}\text{H}_{172}$: C, 89.72; H, 10.28. Found: C, 89.60; H, 10.40.

2,7-Bis[2-[2-[2-(2-ethenyl-9,9-di-*n*-octylfluorenyl)ethenyl]-9,9-di-*n*-octylfluorenyl]ethenyl]-9,9-di-*n*-octylfluorene (dE-OFV5). A bright yellowish green solid was obtained in 81% yield. ^1H NMR (CDCl_3 , 300 MHz): δ (ppm) 7.28–7.70 (m, 38 H), 6.82 (dd, 2 H, $J = 10.9 \text{ Hz}$, 17.5 Hz), 5.82 (d, 2 H, $J = 17.6 \text{ Hz}$), 5.27 (d, 2 H, $J = 11.0 \text{ Hz}$), 1.88–2.13 (m, 20 H), 0.95–1.33 (m, 100 H), 0.80 (t, 30 H, $J = 6.9 \text{ Hz}$), 0.53–0.75 (m, 20 H). Anal. Calcd for $\text{C}_{157}\text{H}_{214}$: C, 89.74; H, 10.26. Found: C, 89.70; H, 10.43.

The Compound dE-OFV7. A bright yellowish green solid was obtained in 71% yield. ^1H NMR (CDCl_3 , 300 MHz): δ (ppm) 7.28–7.71 (m, 54 H), 6.81 (dd, 2 H, $J = 10.9 \text{ Hz}$, 17.6 Hz), 5.82 (d, 2 H, $J = 17.6 \text{ Hz}$), 5.27 (d, 2 H, $J = 10.9 \text{ Hz}$), 1.91–2.15 (m, 28 H), 0.95–1.34 (m, 140 H), 0.80 (t, 42 H, $J = 6.9 \text{ Hz}$), 0.55–0.75 (m, 28 H). Anal. Calcd for $\text{C}_{219}\text{H}_{298}$: C, 89.75; H, 10.25. Found: C, 89.57; H, 10.38.

General Procedure for the Synthesis of dF-OFV $_n$ by the Heck Reaction. Into a degassed mixture of dE-OFV $_n$ (1.0 equiv), aryl iodide **1** (2.2 equiv), anhydrous potassium carbonate (2.2 equiv), tetrabutylammonium bromide (2.2 equiv), and $\text{Pd}(\text{OAc})_2$ (0.10 equiv) was added anhydrous DMF (10 mL per gram dE-OFV $_n$). The mixture was stirred at 110°C for 10 h in absence of light and then poured into water (50 mL). The mixture was extracted with dichloromethane ($3 \times 50 \text{ mL}$), and then the organic extracts were washed with brine, dried with anhydrous MgSO_4 , and concentrated. The product was purified on silica gel column with petroleum ether/dichloromethane as the eluent.

2,7-Bis[2-(2-formyl-9,9-di-*n*-octylfluorenyl)ethenyl]-9,9-di-*n*-octylfluorene (dF-OFV3). A bright yellowish green solid was obtained in 81% yield. ^1H NMR (CDCl_3): δ (ppm) 10.07 (s, 2 H), 7.31–7.91 (m, 22 H), 1.92–2.20 (m, 12 H), 0.94–1.37 (m, 60 H), 0.81 (t, 18 H, $J = 7.2 \text{ Hz}$), 0.49–0.77 (m, 12 H). Anal. Calcd for $\text{C}_{93}\text{H}_{126}\text{O}_2$: C, 87.54; H, 9.95. Found: C, 87.34; H, 10.19. m/z [MALDI-TOF]: 1275.79 (MH^+).

1,2-Bis[2-[2-(2-formyl-9,9-di-*n*-octylfluorenyl)ethenyl]-9,9-di-*n*-octylfluorenyl]ethene (dF-OFV4). A bright yellowish green solid was obtained in 80% yield. ^1H NMR (CDCl_3 , 300 MHz): δ (ppm) 10.07 (s, 2 H), 7.29–7.93 (m, 38 H), 1.93–2.16 (m, 16 H), 0.94–1.31 (m, 80 H), 0.80 (t, 24 H, $J = 6.6 \text{ Hz}$), 0.50–0.74 (m, 16 H). Anal. Calcd for $\text{C}_{124}\text{H}_{168}\text{O}_2$: C, 88.09; H, 10.02. Found: C, 87.89; H 10.24. m/z [MALDI-TOF] 1690.14 (MH^+).

2,7-Bis[2-[2-[2-(2-formyl-9,9-di-*n*-octylfluorenyl)ethenyl]-9,9-di-*n*-octylfluorenyl]ethenyl]-9,9-di-*n*-octylfluorene (dF-OFV5). A bright yellowish green solid was obtained in 76% yield. ^1H NMR (CDCl_3 , 300 MHz): δ (ppm) 10.07 (s, 2 H), 7.30–7.89 (m, 30 H), 1.91–2.15 (m, 20 H), 0.93–1.33 (m, 100 H), 0.81 (t, 30 H, $J = 6.6 \text{ Hz}$), 0.52–0.75 (m, 20 H). Anal. Calcd for $\text{C}_{155}\text{H}_{210}\text{O}_2$: C,

88.43; H, 10.05. Found: C, 88.58; H, 10.19. m/z [MALDI-TOF] 2104.47 (MH^+).

The compound **dF-OFV6**. An orange solid was obtained in 91% yield. 1H NMR ($CDCl_3$, 300 MHz): δ (ppm) 10.07 (s, 2 H), 7.29–7.89 (m, 46 H), 1.89–2.17 (m, 24 H), 0.93–1.34 (m, 120 H), 0.80 (t, 36 H, $J = 6.9$ Hz), 0.49–0.74 (m, 24 H). Anal. Calcd for $C_{186}H_{252}O_2$: C, 88.65; H, 10.08. Found: C, 88.31; H, 10.18. m/z [MALDI-TOF]: 2519.74 (MH^+).

The compound **dF-OFV7**. A bright yellowish green solid was obtained in 66% yield. 1H NMR ($CDCl_3$, 300 MHz): δ (ppm) 10.07 (s, 2 H), 7.29–7.88 (m, 54 H), 1.89–2.17 (m, 28 H), 0.92–1.35 (m, 140 H), 0.80 (t, 42 H, $J = 6.9$ Hz), 0.51–0.75 (m, 28 H). Anal. Calcd for $C_{217}H_{294}O_2$: C, 88.81; H, 10.10. Found: C, 88.86; H, 10.23. m/z [MALDI-TOF]: 2933.93 (MH^+).

The Compound **dF-OFV9**. A bright yellowish green solid was obtained in 68% yield. 1H NMR ($CDCl_3$, 300 MHz): δ (ppm) 10.10 (s, 2 H), 7.47–7.93 (m, 54 H), 7.27–7.33 (m, 16 H), 1.86–2.17 (m, 36 H), 0.93–1.33 (m, 180 H), 0.80 (t, 54 H, $J = 6.8$ Hz), 0.51–0.75 (m, 36 H). Anal. Calcd for $C_{279}H_{388}O_2$: C, 89.03; H, 10.12. Found: C, 88.88; H, 10.34. m/z [MALDI-TOF]: 3763.68 (MH^+).

General Procedure for Synthesis of OFV n by Horner–Wadsworth–Emmons Reaction. Into a solution of **dF-OFV n** (1 equiv) and phosphonate **2** (3 equiv) in anhydrous THF (10–20 mL THF per mmol formyl group) was added a solution of *t*-BuOK (6 equiv, 1.0 M in THF) dropwise at 0 °C. The mixture was stirred at room temperature until the reaction was over, as detected by thin-layer chromatography (TLC), and then poured into water (50 mL). The yellow solid was collected by filtration, washed with ethanol, and then redissolved in CH_2Cl_2 . The solution was dried with anhydrous $MgSO_4$ and concentrated. The product was purification on silica gel column with petroleum ether/dichloromethane as eluent.

2,7-Bis[2-(9,9-di-*n*-octylfluorenyl)ethenyl]-9,9-di-*n*-octylfluorene (OFV3). A bright yellowish green solid was obtained in 88% yield. 1H NMR ($CDCl_3$, 300 MHz): δ (ppm) 7.65–7.74 (m, 6 H), 7.48–7.58 (m, 8 H), 7.27–7.38 (m, 10 H), 1.92–2.13 (m, 12 H), 0.93–1.35 (m, 60 H), 0.81 (t, 18 H, $J = 6.9$ Hz), 0.52–0.74 (m, 12 H). Anal. Calcd for $C_{91}H_{126}$: C, 89.59; H, 10.41. Found: C, 89.44; H, 10.45. m/z [MALDI-TOF]: 1219.94 (MH^+).

1,2-Bis[2-(2-(9,9-di-*n*-octylfluorenyl)ethenyl)-9,9-di-*n*-octylfluorenyl]ethene (OFV4). A bright yellowish green solid was obtained in 88% yield. 1H NMR ($CDCl_3$, 300 MHz): δ (ppm) 7.26–7.73 (m, 40 H), 1.90–2.14 (m, 16 H), 0.94–1.36 (m, 80 H), 0.81 (t, 24 H, $J = 6.9$ Hz), 0.52–0.73 (m, 16 H). Anal. Calcd for $C_{122}H_{168}$: C, 89.64; H, 10.36. Found: C, 89.44; H, 10.56. m/z [MALDI-TOF]: 1634.19 (MH^+).

2,7-Bis[2-(2-(9,9-di-*n*-octylfluorenyl)ethenyl)-9,9-di-*n*-octylfluorenyl]ethenyl]-9,9-di-*n*-octylfluorene (OFV5). A bright yellowish green solid was obtained in 75% yield. 1H NMR ($CDCl_3$, 300 MHz): δ (ppm) 7.57–7.75 (m, 32 H), 7.33–7.47 (m, 8 H), 2.06–2.21 (m, 20 H), 1.05–1.29 (m, 100 H), 0.84 (t, 30 H, $J = 6.6$ Hz), 0.62–0.80 (m, 20 H). Anal. Calcd for $C_{153}H_{210}$: C, 89.67; H, 10.33. Found: C, 89.43; H, 10.35. m/z [MALDI-TOF]: 2049.57 (MH^+).

Oligomer OFV6. A bright yellowish green solid was obtained in 80% yield. 1H NMR ($CDCl_3$, 300 MHz): δ (ppm) 7.27–7.74 (m, 48 H), 1.91–2.17 (m, 24 H), 0.96–1.35 (m, 120 H), 0.80 (t, 36 H, $J = 6.9$ Hz), 0.56–0.74 (m, 24 H). ^{13}C NMR ($CDCl_3$, 75 MHz): δ (ppm) 151.9, 151.7, 151.4, 141.3, 141.0, 136.9, 129.0, 127.4, 127.2, 126.1, 123.3, 121.0, 120.3, 120.0, 55.43, 41.09, 40.93, 32.20, 30.51, 29.64, 24.17, 22.98, 14.45. Anal. Calcd for $C_{184}H_{252}$: C, 89.69; H, 10.31. Found: C, 89.44; H, 10.57. m/z [MALDI-TOF]: 2463.89 (MH^+).

Oligomer OFV7. A bright yellowish green solid was obtained in 77% yield. 1H NMR ($CDCl_3$, 300 MHz): δ (ppm) 7.57–7.75 (m, 44 H), 7.33–7.44 (m, 12 H), 1.95–2.22 (m, 28 H), 1.10–1.28 (m, 140 H), 0.84 (t, 42 H, $J = 5.5$ Hz), 0.62–0.79 (m, 28 H). ^{13}C NMR ($CDCl_3$, 75 MHz): δ (ppm) 152.0, 151.7, 151.4, 141.3, 141.1, 136.9, 129.0, 127.4, 127.2, 126.1, 123.3, 121.0, 120.3, 120.0, 55.44, 41.11, 40.95, 32.21, 30.52, 29.65, 24.19, 23.00, 14.46. Anal. Calcd

for $C_{215}H_{294}$: C, 89.71; H, 10.29. Found: C, 89.46; H, 10.55. m/z [MALDI-TOF]: 2879.17 (MH^+).

Oligomer OFV8. A bright yellowish green solid was obtained in 78% yield. 1H NMR ($CDCl_3$, 300 MHz): δ (ppm) 7.26–7.73 (m, 64 H), 1.89–2.19 (m, 32 H), 0.97–1.35 (m, 160 H), 0.80 (t, 48 H, $J = 6.9$ Hz), 0.54–0.74 (m, 32 H). ^{13}C NMR ($CDCl_3$, 75 MHz): δ (ppm) 151.9, 151.7, 151.4, 141.3, 141.1, 136.9, 129.0, 127.4, 127.2, 126.1, 123.2, 121.0, 120.3, 120.0, 55.43, 41.10, 40.93, 32.20, 30.51, 29.64, 24.18, 22.99, 14.45. Anal. Calcd for $C_{246}H_{336}$: C, 89.72; H, 10.28; Found: C, 89.45; H, 10.27. m/z [MALDI-TOF]: 3293.51 (MH^+).

Oligomer OFV9. A greenish yellow solid was obtained in 61% yield. 1H NMR ($CDCl_3$, 300 MHz): δ (ppm) 7.27–7.75 (m, 72 H), 1.82–2.27 (m, 36 H), 0.96–1.39 (m, 180 H), 0.80 (t, 54 H, $J = 6.9$ Hz), 0.52–0.74 (m, 36 H). ^{13}C NMR ($CDCl_3$, 75 MHz): δ (ppm) 151.9, 151.6, 151.4, 141.3, 140.0, 136.9, 129.0, 127.4, 127.2, 126.1, 123.2, 121.0, 120.3, 120.0, 55.43, 41.10, 40.94, 32.20, 30.50, 29.64, 24.18, 22.98, 14.45. Anal. Calcd for $C_{277}H_{378}$: C, 89.72; H, 10.28. Found: C, 89.34; H, 10.36. m/z [MALDI-TOF]: 3708.89 (MH^+).

Oligomer OFV11. A greenish yellow solid was obtained in 86% yield. 1H NMR ($CDCl_3$, 300 MHz): δ (ppm) 7.64–7.75 (m, 22 H), 7.49–7.60 (m, 40 H), 7.27–7.44 (m, 26 H), 2.00–2.19 (m, 44 H), 0.94–1.31 (m, 220 H), 0.81 (t, $J = 6.9$ Hz, 66 H), 0.51–0.73 (m, 44 H). ^{13}C NMR ($CDCl_3$, 75 MHz): δ (ppm) 151.9, 151.7, 151.4, 141.3, 141.0, 136.9, 129.0, 127.4, 121.2, 126.1, 123.2, 121.0, 120.3, 120.0, 55.43, 41.10, 40.94, 32.20, 30.50, 29.64, 24.17, 22.99, 14.45. Anal. Calcd for $C_{339}H_{462}$: C, 89.72; H, 10.28. Found: C, 89.88; H, 10.28. m/z [MALDI-TOF]: 4538.03 (MH^+).

Measurements. 1H NMR and ^{13}C NMR spectra were recorded on a Bruker AV 300 spectrometer at 300 MHz using $CDCl_3$ as the solvent. Element analysis was performed on a FlashEA1112 elemental analysis system. MALDI-TOF mass spectra were recorded on a Kratos AXIMA-CFR Kompact MALDI mass spectrometer with 2,5-dihydroxybenzoic acid (DHB) as the matrix. GPC measurements were conducted on a Waters 510 system equipped with a Waters 410 Differential refractometer and a WATO44027 column using polystyrene as standard and THF as the eluent. The nature of the phase transition was characterized with an Olympus BX51 polarizing optical microscope equipped with a LTS 350 hot stage and a TMS 94 temperature programmer (Linkam). Differential scanning calorimetry (DSC) was run on a TA Instruments Q100 DSC under flow of N_2 at heating/cooling rates of 10 °C·min $^{-1}$. The heating temperature limit was selected based on POM observation to be at least 20 °C higher than the temperature above which the oligomer was isotropic. UV-vis absorption and PL spectra were recorded on a Perkin-Elmer Lambda 35 UV-vis spectrometer and a Perkin-Elmer LS 50B luminescence spectrometer, respectively. All films for absorption and PL measurements were spin-coated at 1500 rpm for 1 min with the solution concentration of 8 mg·mL $^{-1}$.

Cyclic voltammetry (CV) was performed on a CHI660a electrochemical analyzer with a three-electrode cell in a solution of 0.1 mol·L $^{-1}$ tetrabutylammonium hexafluorophosphate (Bu_4NPF_6) in anhydrous CH_2Cl_2 at a scan rate of 20 mV·s $^{-1}$. The oligomer concentration was 1×10^{-3} mol·L $^{-1}$ of repeating unit. A platinum (Pt) electrode with a diameter of 2 mm, a Pt wire, and an Ag/AgCl electrode were used as the working electrode, the counter electrode, and the reference electrode, respectively. The potential was calibrated against the ferrocene/ferrocenium couple (0.44 V vs Ag/AgCl in CH_2Cl_2). HOMO energy levels were estimated by the equation: HOMO = $-(4.36 + E_{\text{oxd onset}})$.²¹ Electroluminescence devices were fabricated and characterized following a previous publication.²²

Acknowledgment. This work is supported by the NSFC (Nos. 20423003, 20474063, and 20521415), the Science Fund for Creative Research Groups of NSFC (20621401), the Hundreds Talents Program of Chinese Academy of Sciences, and the Distinguished Young Scholar Foundation of Jilin Province (No.20040101).

Supporting Information Available: Text and a scheme detailing the synthesis of intermediates and **OFV2** and figures showing GPC profiles and representative CV curves of **OFV_n**. This material is available free of charge via the Internet at <http://pubs.acs.org>.

References and Notes

- (1) (a) Friend, R. H.; Gymer, R. W.; Holmes, A. B.; Burroughes, J. H.; Marks, R. N.; Taliani, C.; Bradley, D. D. C.; Dos Santos, D. A.; Brédas, J. L.; Lögdlund, M.; Salaneck, W. R. *Nature (London)* **1999**, *397*, 121–128. (b) Kim, D. Y.; Cho, H. N.; Kim, C. Y. *Prog. Polym. Sci.* **2000**, *25*, 1089–1139. (c) Akcelrud, L. *Prog. Polym. Sci.* **2003**, *28*, 875–962. (d) Kraft, A.; Grimsdale, A. C.; Holmes, A. B. *Angew. Chem., Int. Ed.* **1998**, *37*, 402–428. (e) Neher, D. *Macromol. Rapid Commun.* **2001**, *22*, 1365–1385.
- (2) (a) Mikroyannidis, J. A.; Yu, Y.-J.; Lee, S.-H.; Jin, J.-I. *J. Polym. Sci., Part A: Polym. Chem.* **2006**, *44*, 4494–4507. (b) Cho, H. N.; Kim, D. Y.; Kim, J. K.; Kim, C. Y. *Synth. Met.* **1997**, *91*, 293–296.
- (3) (a) Hwang, D.-H.; Lee, J.-D.; Kang, J.-M.; Lee, S.; Lee, C.-H.; Jin, S.-H. *J. Mater. Chem.* **2003**, *13*, 1540–1545. (b) Jin, S.-H.; Kang, S. Y.; Kim, M.-Y.; Chan, Y.-U.; Kim, J.-Y.; Lee, K.; Gal, Y.-S. *Macromolecules* **2003**, *36*, 3841–3847. (c) Jin, S.-H.; Park, H.-J.; Kim, J.-Y.; Lee, K.; Lee, S.-P.; Moon, D.-K.; Lee, H.-J.; Gal, Y.-S. *Macromolecules* **2002**, *35*, 7532–7534.
- (4) Anuragudom, P.; Newaz, S. S.; Phanichphant, S.; Lee, T. R. *Macromolecules* **2006**, *39*, 3494–3499.
- (5) Nomura, K.; Morimoto, H.; Imanishi, Y.; Ramhani, Z.; Geerts, Y. J. *Polym. Sci., Part A: Polym. Chem.* **2001**, *39*, 2463–2470.
- (6) (a) Martin, R. E.; Diederich, F. *Angew. Chem., Int. Ed.* **1999**, *38*, 1350–1377. (b) Müllen, K.; Wegner, G. *Electronic Materials: The Oligomer Approach*; Wiley-VCH: Weinheim, Germany, and New York, 1998. (c) Schwab, P. F. H.; Smith, J. R.; Michl, J. *Chem. Rev.* **2005**, *105*, 1197–1279.
- (7) (a) Meier, H. *Angew. Chem., Int. Ed.* **2005**, *44*, 2482–2506. (b) Hoebe, F. J. M.; Jonkheijm, P.; Meijer, E. W.; Schenning, A. P. H. *J. Chem. Rev.* **2005**, *105*, 1491–1546. (c) Schenning, A. P. H. J.; Meijer, E. W. *Chem. Commun.* **2005**, 3245–3258. (d) Carroll, R. L.; Gorman, C. B. *Angew. Chem., Int. Ed.* **2002**, *41*, 4378–4400. (e) Meier, H.; Stalmach, U.; Kolshorn, H. *Acta Polym.* **1997**, *48*, 379–384.
- (8) (a) Geng, Y. H.; Trajkovska, A.; Katsis, D.; Ou, J. J.; Culligan, S. W.; Chen, S. H. *J. Am. Chem. Soc.* **2002**, *124*, 8337–8347. (b) Geng, Y. H.; Culligan, S. W.; Trajkovska, A.; Wallace, J. U.; Chen, S. H. *Chem. Mater.* **2003**, *15*, 542–549.
- (9) (a) Izumi, T.; Kobashi, S.; Takimiya, K.; Aso, Y.; Otsubo, T. *J. Am. Chem. Soc.* **2003**, *125*, 5286–5287. (b) Nakanishi, H.; Sumi, N.; Aso, Y.; Otsubo, T. *J. Org. Chem.* **1998**, *63*, 8632–8633.
- (10) (a) Pearson, D. L.; Tour, J. M. *J. Org. Chem.* **1997**, *62*, 1376–1387. (b) Jones, L.; Schumm, J. S.; Tour, J. M. *J. Org. Chem.* **1997**, *62*, 1388–1410.
- (11) (a) Eisler, S.; Slepko, A. D.; Elliott, E.; Luu, T.; McDonald, R.; Hegmann, F. A.; Tykewinski, R. R. *J. Am. Chem. Soc.* **2005**, *127*, 2666–2676. (b) Gibtnier, T.; Hampel, F.; Gisselbrecht, J.-P.; Hirsch, A. *Chem.—Eur. J.* **2002**, *8*, 408–432.
- (12) (a) Wang, H.; Wang, H. H.; Urban, V. S.; Littrell, K. C.; Thiyagarajan, P.; Yu, L. *J. Am. Chem. Soc.* **2000**, *122*, 6855–6861. (b) Gebhardt, V.; Bacher, A.; Thelakktat, M.; Stalmach, U.; Meier, H.; Schmidt, H.-W.; Haarer, D. *Adv. Mater.* **1999**, *11*, 119–123. (c) Roncali, J. *Acc. Chem. Res.* **2000**, *33*, 147–156.
- (13) Liess, P.; Hensel, V.; Schluter, A. D. *Liebigs Ann.* **1996**, 1037–1040.
- (14) (a) Culligan, S. W.; Geng, Y. H.; Chen, S. H.; Klubek, K.; Vaeth, K. M.; Tang, C. W. *Adv. Mater.* **2003**, *15*, 1176–1180. (b) Yasuda, T.; Fujita, K.; Tsutsui, T.; Geng, Y. H.; Culligan, S. W.; Chen, S. H. *Chem. Mater.* **2005**, *17*, 264–268.
- (15) (a) Jo, J.; Chi, C.; Höger, S.; Wegner, G.; Yoon, D. Y. *Chem.—Eur. J.* **2004**, *10*, 2681–2688. (b) Somma, E.; Loppinet, B.; Chi, C.; Fytas, G.; Wegner, G. *Phys. Chem. Chem. Phys.* **2006**, *8*, 2773–2778.
- (16) Lee, S. H.; Nakamura, T.; Tsutsui, T. *Org. Lett.* **2001**, *3*, 2005–2007.
- (17) Wang, S.; Oldham, W. J.; Hudack, R. A.; Bazan, G. C. *J. Am. Chem. Soc.* **2000**, *122*, 5695–5709.
- (18) Grell, M.; Bradley, D. D. C.; Long, X.; Chamberlain, T.; Inbasekaran, M.; Woo, E. P.; Soliman, M. *Acta Polym.* **1998**, *49*, 439–444.
- (19) Jiang, X. Z.; Liu, S.; Liu, M. S.; Herguth, P.; Jen, A. K. Y.; Fong, H.; Sarikaya, M. *Adv. Func. Mater.* **2002**, *12*, 745–751.
- (20) Birks, J. B.; Dyson, D. J. *Proc. R. Soc. London, Ser. A* **1963**, *275*, 135–148.
- (21) Bard, A. J.; Faulkner, L. A. *Electrochemical Methods-Fundamentals and Applications*; Wiley: New York 1984.
- (22) Jiang, G.; Yao, B.; Geng, Y. H.; Cheng, Y.; Xie, Z.; Wang, L.; Jing, X.; Wang, F. *Macromolecules* **2006**, *39*, 1403–1409.

MA0628073